


ORIGINAL ARTICLE

Therapeutic potential of deuterium-stabilized (*R*)-pioglitazone—PXL065—for X-linked adrenoleukodystrophy

Pierre-Axel Monternier¹ | Jaspreet Singh² | Parveen Parasar² |
 Pierre Theurey¹  | Sheila DeWitt³ | Vincent Jacques³ | Eric Klett⁴ |
 Navtej Kaur² | Tavarekere N. Nagaraja⁵ | David E. Moller¹ |
 Sophie Hallakou-Bozec¹

¹Poxel SA, Lyon, France

²Department of Neurology, Henry Ford Health System, Detroit, Michigan, USA

³DeuteRx, LLC, Andover, Massachusetts, USA

⁴Department of Medicine, Division of Endocrinology, University of North Carolina School of Medicine, Chapel Hill, North Carolina, USA

⁵Department of Neurosurgery, Henry Ford Health System, Detroit, Michigan, USA

Correspondence

Pierre Theurey, Poxel SA, 259 Av. Jean Jaurès, 69007 Lyon, France.
 Email: pierre.theurey@poxelpharma.com

Funding information

Henry Ford Health System; National Institute of Health, USA, Grant/Award Numbers: NS114775, NS114245; Poxel

Abstract

X-linked adrenoleukodystrophy (ALD) results from ABCD1 gene mutations which impair Very Long Chain Fatty Acids (VLCFA; C26:0 and C24:0) peroxisomal import and β -oxidation, leading to accumulation in plasma and tissues. Excess VLCFA drives impaired cellular functions (e.g. disrupted mitochondrial function), inflammation, and neurodegeneration. Major disease phenotypes include: adrenomyeloneuropathy (AMN), progressive spinal cord axonal degeneration, and cerebral ALD (C-ALD), inflammatory white matter demyelination and degeneration. No pharmacological treatment is available to-date for ALD. Pioglitazone, an anti-diabetic thiazolidinedione, exerts potential benefits in ALD models. Its mechanisms are genomic (PPAR γ agonism) and nongenomic (mitochondrial pyruvate carrier—MPC, long-chain acyl-CoA synthetase 4—ACSL4, inhibition). However, its use is limited by PPAR γ -driven side effects (e.g. weight gain, edema). PXL065 is a clinical-stage deuterium-stabilized (*R*)-enantiomer of pioglitazone which lacks PPAR γ agonism but retains MPC activity. Here, we show that incubation of ALD patient-derived cells (both AMN and C-ALD) and glial cells from *Abcd1*-null mice with PXL065 resulted in: normalization of elevated VLCFA, improved mitochondrial function, and attenuated indices of inflammation. Compensatory peroxisomal transporter gene expression was also induced. Additionally, chronic treatment of *Abcd1*-null mice lowered VLCFA in plasma, brain and spinal cord and improved both neural histology (sciatic nerve) and neurobehavioral test performance. Several *in vivo* effects of PXL065 exceeded those achieved with pioglitazone. PXL065 was confirmed to lack PPAR γ agonism but retained ACSL4 activity of pioglitazone. PXL065 has novel actions

[Click here to access the podcast for this paper.](#)

Pierre-Axel Monternier, Jaspreet Singh, David E. Moller, and Sophie Hallakou-Bozec contributed equally to this study.

This is an open access article under the terms of the [Creative Commons Attribution](#) License, which permits use, distribution and reproduction in any medium, provided the original work is properly cited.

© 2022 Poxel SA. *Journal of Inherited Metabolic Disease* published by John Wiley & Sons Ltd on behalf of SSIEM.

and mechanisms and exhibits a range of potential benefits in ALD models; further testing of this molecule in ALD patients is warranted.

1 | INTRODUCTION

X-linked adrenoleukodystrophy (ALD) is a rare neuro-metabolic disease caused by mutations in the ATP Binding Cassette subfamily D, member 1 (ABCD1) gene. These mutations lead to impaired function of the adrenoleukodystrophy Protein (ALDP), preventing the transport of Very Long Chain Fatty Acids (VLCFA) into peroxisomes.¹ As VLCFA cannot enter the peroxisomes to be oxidized, they accumulate in plasma² and tissues.¹ Thus, increased circulating and tissue levels of VLCFA, in particular saturated C26 (C26:0) and C24 (C24:0), have been described as the hallmark of the pathology. Importantly, elevated cellular C26:0 levels are established as the proximate cause of disease^{3,4} and are believed to be responsible for oxidative stress, inflammation, and mitochondrial dysfunction, leading to neuronal atrophy and demyelination.^{5–7}

There are two main clinical subtypes of ALD. Adrenomyeloneuropathy (AMN) is an adult, slowly progressive disease leading to severe disabilities. Its pathophysiology is characterized by spinal cord and peripheral nerve degeneration that lead to spastic paraparesis and sensory ataxia.¹ The second main form, cerebral ALD (C-ALD), typically occurs during childhood (but also in adults) and is characterized by brain white matter lesions and the rapid progression of neurologic deficits and death, caused by a rapid inflammatory demyelination process.⁸

Although allogeneic hematopoietic stem cell transplantation is now employed to treat early-stage C-ALD, there is currently no approved pharmacologic treatment available for AMN or C-ALD. Hence, it is critically important to investigate potential therapeutics that could either halt the progression of AMN or treat and prevent the onset of C-ALD.

Pioglitazone—a marketed antidiabetic thiazolidinedione (TZD) drug—improved the disease phenotype of *Abcd1*-null mice by normalizing bioenergetic parameters and decreasing oxidative stress in spinal cord and ameliorating impaired locomotor function.⁹ Additionally, leriglitazone, a related TZD (the M-IV metabolite of pioglitazone), which is currently under development for ALD, also exhibited an encouraging preclinical profile suggesting that this class of compounds is of high interest to treat ALD.¹⁰ The efficacy observed to-date with both pioglitazone and leriglitazone has been attributed to transcriptional actions as agonists of peroxisome proliferator activated receptor γ (PPAR γ).^{9,10}

Pioglitazone is a racemic mixture of interconverting (*R*)- and (*S*)-enantiomers. We recently discovered that only the (*S*)-enantiomer exerts potent PPAR γ activity, whereas both the (*R*)- and (*S*)-enantiomers (and the parent racemate) have other—nongenomic—actions.¹¹ PXL065 is a stabilized form of (*R*)-pioglitazone created by the addition of deuterium to its chiral center.¹¹ In cell culture and in vivo, PXL065 retains pioglitazone's nongenomic activity with substantially less PPAR γ agonism, the latter leading to undesired TZD side effects (body weight gain and edema).

Here, we investigated the effects of PXL065 on hallmarks of ALD in both in vitro and in vivo models. In diseased patient-derived cells, multiple beneficial effects on cellular phenotypes, including correction of elevated VLCFA, were documented. In addition, chronic administration of PXL065 to *Abcd1*-null mice produced distinct reductions in plasma and tissue VLCFA accumulation along with improvements in other disease-associated phenotypes. As PXL065 has recently completed Phase I trials in healthy subjects, the clinical trial assessment of its potential effects in patients with ALD (adult male AMN) is planned to initiate in 2022.

2 | MATERIAL AND METHODS

2.1 | In vitro studies

2.1.1 | Work system

Compounds

PXL065 was synthesized by AAPharmaSyn; pioglitazone was purchased from Dr. Reddy's Laboratories (India); compounds were dissolved in DMSO.

Human-derived cells

Primary human fibroblasts (healthy: GM03348, AMN: GM17819, C-ALD: GM04934), and immortalized human lymphocytes (healthy: GM03798, C-ALD: GM04673) were obtained from the NIGMS Human Genetic Cell Repository, Coriell Institute for Medical Research (www.coriell.org) and cultured as previously described.¹²

Mouse-derived glial cells

Mouse primary mixed glial cells were prepared from 2-day-old wild-type (WT) and *Abcd1* null pups, as previously described.¹³

2.1.2 | mRNA levels

0.5 million cells/well were plated in 6-well plates. After 72 h of compound exposure (cells at 80% confluence), mRNA was isolated (Qiagen RNAeasy kit, #74104) and cDNA was prepared (Qiagen RT II cDNA kit [Qiagen, #330401]). Real-time quantitative polymerase chain reaction (PCR) was conducted using Bio-Rad CFX96 Real-Time PCR Detection System and iTaq™ Universal SYBR® Green Supermix (Bio-Rad, #1725124). Results are expressed as ratio of the targeted gene over the house-keeping gene, RLP27.

2.1.3 | VLCFA content

300 K cells were plated in 100-mm petri plates. Cells were treated for 7 days. At the end of treatment (cells at 80% confluence), cells were washed with ice-cold phosphate buffered saline and 1 million cells per sample were pelleted and provided to the Lipidomic Core for VLCFA analysis as described in Appendix S1.

2.1.4 | Bioenergetics

0.5 million cells/well were plated in 6-well plates. Cells were treated for 72 h (cells at 80% confluence at the end of treatment). They were then harvested with cell lifters and washed twice with bicarbonate-free DMEM prewarmed at 37°C. 1 million cells/well were plated in 175 µl of bicarbonate-free DMEM in XF96 plates and preincubated at 37°C for 1 h for degassing. Oxygen consumption rate (OCR) was measured using Seahorse XF96 Analyzer (Agilent) as previously described.¹²

2.1.5 | Long-chain acyl-CoA synthetase (ACS) activity

ACSL enzyme activity assays were performed using purified recombinant rat FLAG-ACSL1 and FLAG-ACSL4 with [¹⁴C] palmitate and a scintillation counter as described in Appendix S1.

2.2 | PPAR γ agonist assay

PPAR γ agonist activity was measured using histidine-tagged-PPAR γ , biotin-tagged-TRAP220 coactivator and fluorescence acceptor/donor as described in Appendix S1. The results are expressed as a percent of the control response to 10 µM rosiglitazone.

2.3 | Inflammatory gene expression profiling

C-ALD patient-derived lymphocytes were cultured in Serum-free DMEM for cytokine mRNA analysis for 72 h. Abcd1-null glial cells were cultured in serum-free media overnight followed by 2 h pretreatment with tested compounds; TNF α (10 ng/ml) and IL1 β (10 ng/ml) were then added to the media for 70 h resulting in a total compound exposure period of 72 hrs. mRNA levels were measured as described above.

2.4 | In vivo experiments

2.4.1 | Animals

Animals were handled following the appropriate ethical guidelines as described in Appendix S1. All institutional and national guidelines for the care and use of laboratory animals were followed. Genotyping was performed by PCR as described in Appendix S1.

2.5 | VLCFA assessment in 6- to 8-week-old and 13-month-old Abcd1-null mice

6- to 8-week-old Abcd1-null male mice were treated with PXL065, pioglitazone (15 mg/kg), or methylcellulose vehicle once daily (QD, oral gavage) for 8 weeks. VLCFA content was measured in plasma, spinal cord, and brain after 8 weeks of treatment. VLCFA content in spinal cord was also assessed in 13-month-old mice treated for 12 weeks with PXL065 or pioglitazone at 15 mg/kg QD. On the last treatment day, mice were sacrificed with CO₂; plasma, brain and spinal cord were then harvested, snap-frozen in liquid nitrogen and stored at -80°C until processed for VLCFA analysis (see above).

2.6 | Behavioral tests in 13-month-old Abcd1-null mice (open-field test)

13-month-old Abcd1-null male mice were treated with compound or vehicle as noted above.

Measures of locomotion and exploration, including total distance, freezing time, and number of rearings, were scored. Data were obtained as described in Appendix S1.

2.7 | Axonal morphology

Electronic microscopy (EM) morphometric studies were performed on thin sections (1 µM) of sciatic nerve from

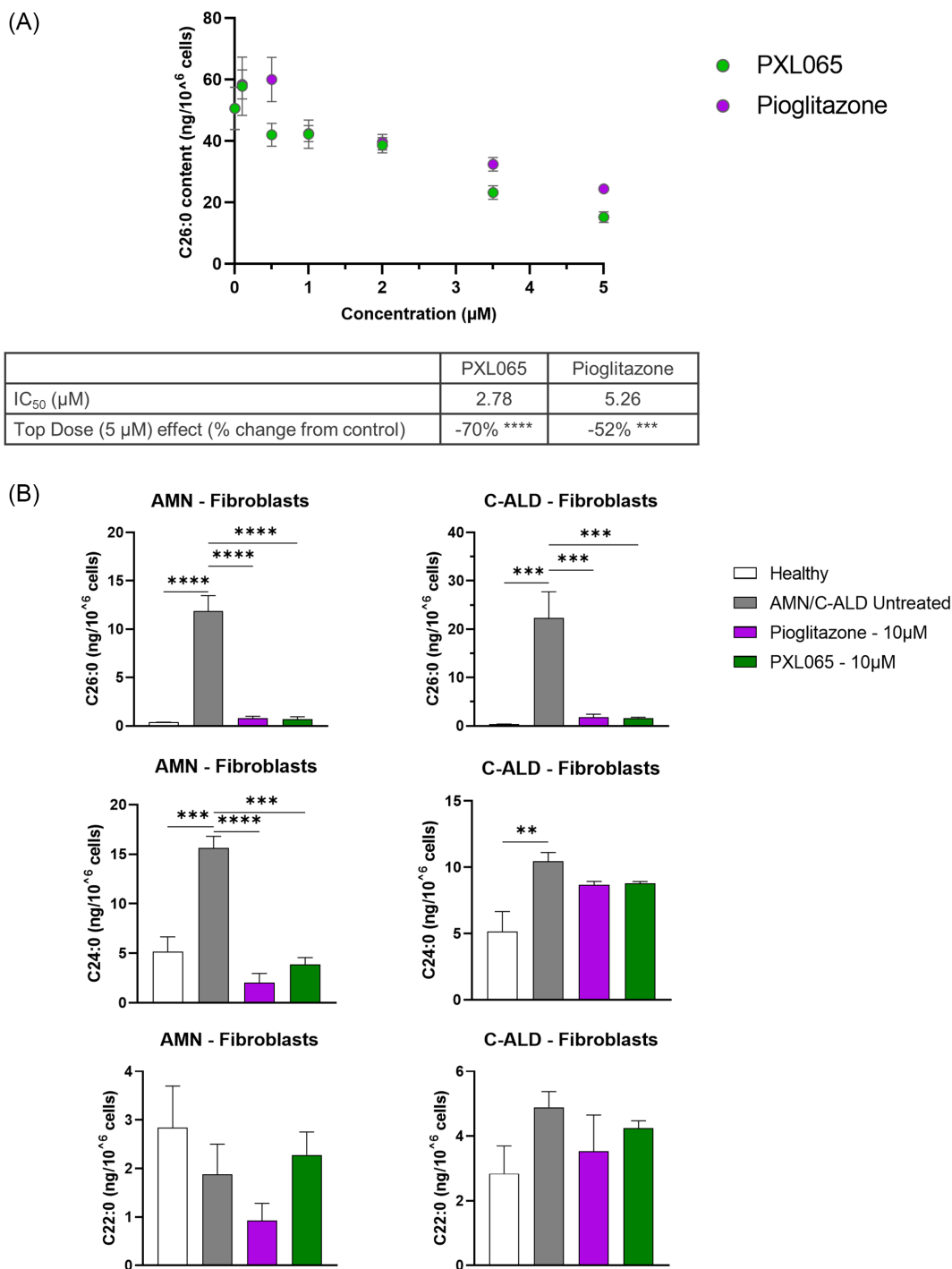


FIGURE 1 PXL065 and Pioglitazone suppress very long chain fatty acids (VLCFA) levels in fibroblasts derived from two adrenoleukodystrophy (ALD)—C-ALD and AMN—patients. (A) Dose–response effect of PXL065, pioglitazone on C26:0 levels measured by mass spectrometry in AMN fibroblasts following incubation with compounds at 0, 0.1, 0.5, 1, 2, 3.5, and 5 µM for 7 days. IC₅₀s were calculated using nonlinear regression analysis. Results are mean ± SEM, *n* = 5 replicates. (B) Effect of PXL065 and pioglitazone on VLCFA levels measured by mass spectrometry in AMN and C-ALD fibroblasts, following incubation at 10 µM for 7 days. Results are mean ± SEM, *n* = 3 replicates/condition/patient. Beneficial effects of the drugs on VLCFA levels were reproduced in fibroblasts derived from these donors in two other independent experiments. ** *p* < 0.01, *** *p* < 0.001, **** *p* < 0.0001 by One-way analysis of variance (ANOVA) followed by Dunnett’s multiple comparison versus untreated AMN/C-ALD cells

WT and Abcd1-null mice, as described in Appendix S1. Criteria for blinded evaluations were appearance of axons, scored as regular and nearly circular bundles or stellate (star-like).

2.8 | Statistics

Data were analyzed using Graph Pad Prism® V9.3.1 software. Analysis was conducted using raw values

including all groups. Model characterization and significance of treatment effects were tested using one-way analysis of variance followed by Dunnett's multiple comparisons test when data were normally distributed, and Kruskal–Wallis followed by Dunn's multiple comparisons test when data were not normally distributed.

3 | RESULTS

3.1 | PXL065 suppresses elevated VLCFA in patient-derived fibroblasts

The dose–response range of PXL065 was determined in AMN patient-derived fibroblasts alongside effects of

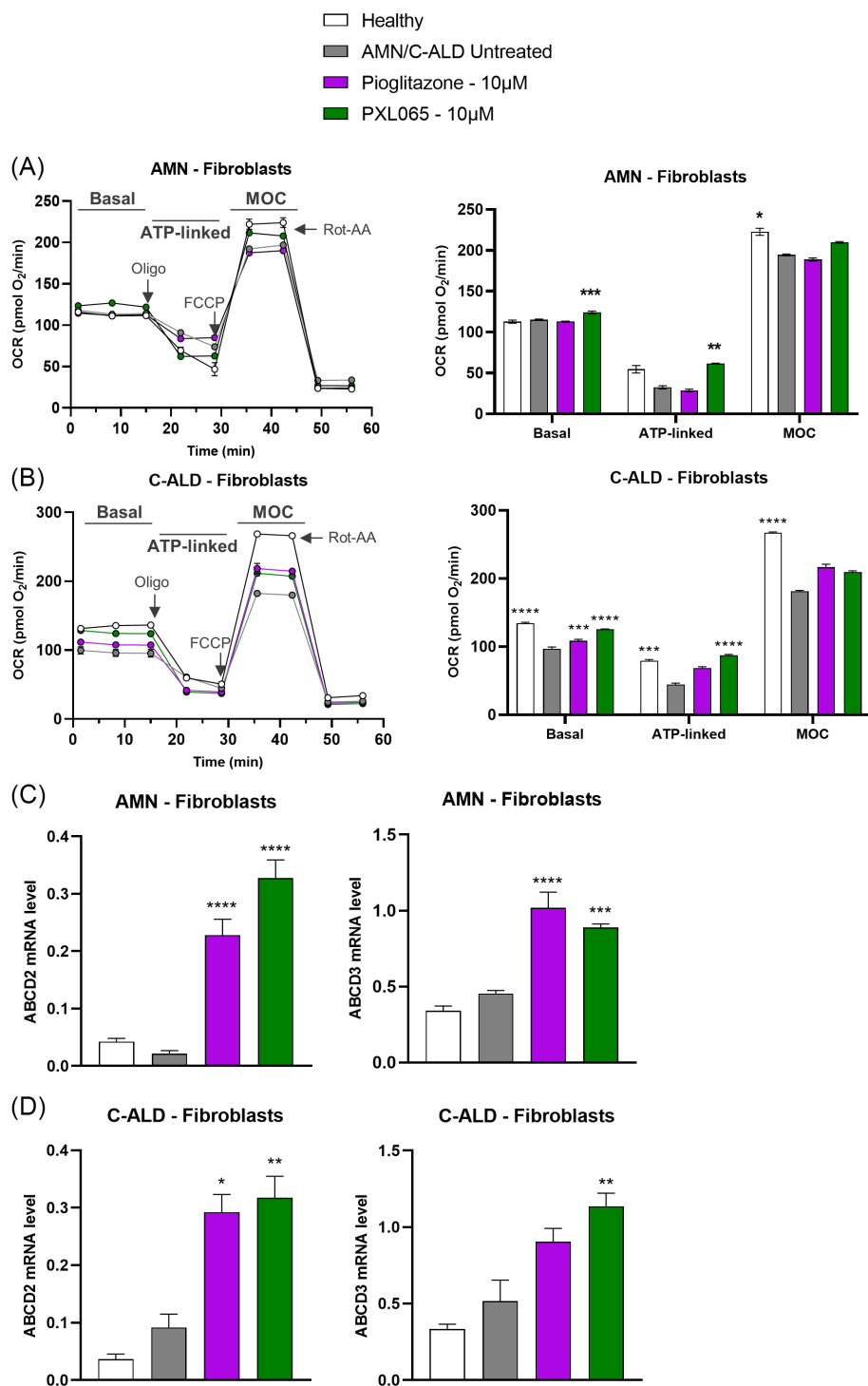


FIGURE 2 PXL065 improves mitochondrial function and increases compensatory transporters, ABCD2 and ABCD3, mRNA levels in fibroblasts derived from two ALD—C-ALD and AMN—patients. AMN (A) and C-ALD (B) fibroblasts were exposed for 72 h to PXL065 or Pioglitazone at 10 µM. Bioenergetics analysis was performed using a Seahorse Analyzer and parameters were evaluated by sequential additions of: oligomycin (Oligo—1 µM), FCCP (0.25 µM) and Rotenone-Antimycin A (Rot-AA—1 µM). Basal is first three measurements, ATP-linked is oxygen consumption rate (OCR) drop following oligo addition, Maximal Oxidative Capacity (MOC) is OCR following addition of FCCP. Results are mean ± SEM, $n = 6$ replicates/condition/patient. Cells were exposed for 72 h to PXL065 or pioglitazone at 10 µM prior to mRNA level analysis by RT-qPCR in AMN (C) and C-ALD fibroblasts (D). Results are mean ± SEM, $n = 3–6$ replicates/condition/patient. * $p < 0.05$, ** $p < 0.01$, *** $p < 0.001$, **** $p < 0.0001$ by One-way analysis of variance followed by Dunnett's multiple comparison versus untreated AMN/C-ALD cells

pioglitazone (Figure 1A). After 7 days of treatment, PXL065 reduced elevated C26:0 in a dose dependent manner ($IC_{50} = 2.78 \mu\text{M}$); pioglitazone had a similar effect with slightly lower potency ($IC_{50} = 5.26 \mu\text{M}$). Additionally, the C26:0/C22:0 ratio was significantly decreased by PXL065 and pioglitazone indicating relative selectivity on VLCFA (data not shown). Following these results, we pursued our investigations with PXL065 in two independent sets of experiments conducted with one cell line obtained from an adult ALD patient (with AMN—"AMN fibroblasts"), and another cell line from a younger ALD patient (with C-ALD—"C-ALD fibroblasts").

In confirmatory experiments also aimed at assessing maximal effects, PXL065 consistently reduced elevated C26:0 and C24:0 levels in AMN fibroblasts (Figure 1B) (-94% , $p < 0.0001$ and -75% , $p < 0.001$, respectively). In C-ALD fibroblasts, PXL065 decreased C26:0 levels (-93% , $p < 0.001$) but not C24:0 when compared to untreated cells (Figure 1B). C22:0 levels (not known to be disease associated) were not elevated—and were unaffected by PXL065—in either AMN or C-ALD cells (Figure 1B). Overall, a similar profile was observed with pioglitazone. The same pattern seen in patient-derived fibroblasts was also observed in lymphocytes treated with PXL065 and pioglitazone (Figure S1).

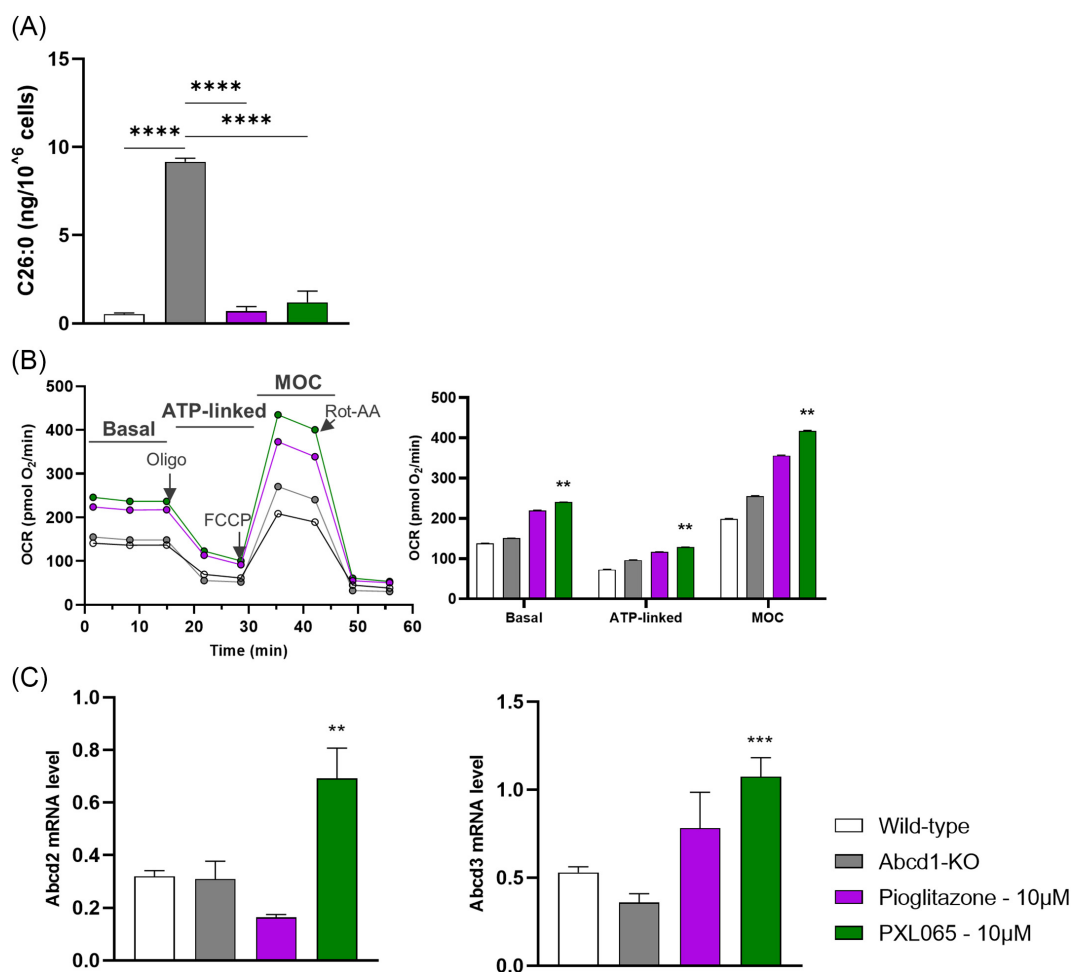


FIGURE 3 PXL065 improves adrenoleukodystrophy (ALD) pathology in glial cells from Abcd1-null mice. Cells were exposed to 10 μM PXL065, pioglitazone, or control media. (A) Very long chain fatty acids (C26:0) quantitative analysis performed by mass spectrometry after 7 days exposure. (B) Bioenergetics analysis performed using a Seahorse Analyzer after 72-h incubation; parameters were evaluated by sequential additions of: oligomycin (Oligo), FCCP and Rotenone-Antimycin A. Basal is first three measurements, ATP-linked is oxygen consumption rate (OCR) drop following oligo addition, Maximal Oxidative Capacity (MOC) is OCR following addition of FCCP. (C) Compensatory transporter gene expression measured by RT-qPCR (normalized by RLP27 expression) after 72-h incubation. Results are mean \pm SEM, $n = 2-6$ replicates/condition. ** $p < 0.01$, *** $p < 0.001$, **** $p < 0.0001$ by one-way analysis of variance followed by Dunnett's multiple comparison versus untreated glial cells

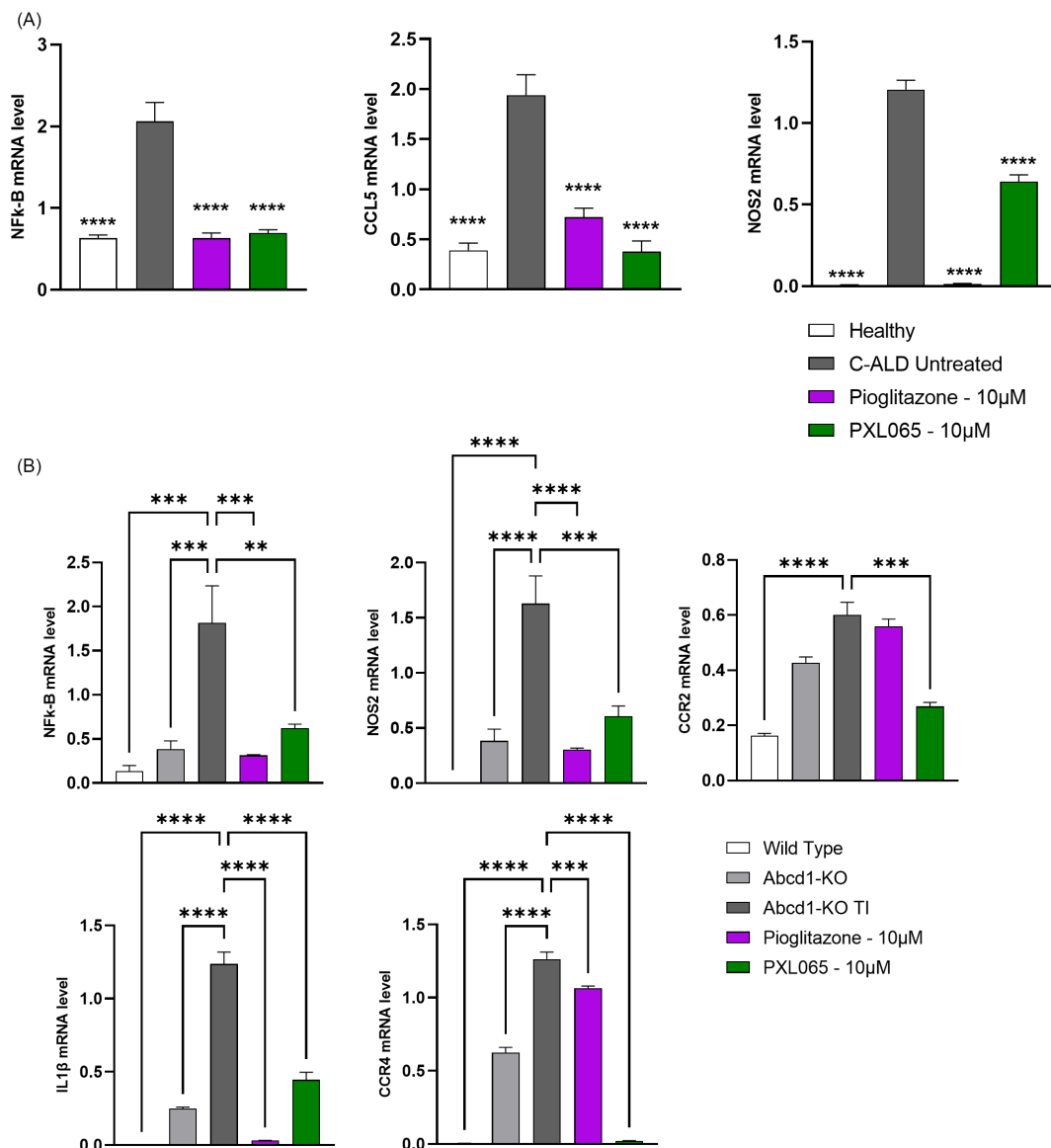


FIGURE 4 PXL065 represses pro-inflammatory gene expression in C-ALD patient-derived lymphocytes and in glial cells from Abcd1-null mice. C-ALD lymphocytes (A) were exposed for 72 h to PXL065 or Pioglitazone at 10 μM prior to mRNA level analysis by RT-qPCR. Abcd1 null glial cells (B) were incubated with PXL065 or Pioglitazone at 10 μM for 2 h prior to stimulation by TNFα and IL1β for 70 h (total drug exposure of 72 h), followed by mRNA level analysis by RT-qPCR. Results are mean ± SEM, $n = 3$ replicates/condition. Results were normalized by RPL27 expression. ** $p < 0.01$, *** $p < 0.001$, **** $p < 0.0001$ by One-way ANOVA followed by Dunnett's multiple comparison vs untreated C-ALD or Abcd1 null glial cells.

3.2 | PXL065 enhances mitochondrial function and induces expression of compensatory fatty acid transporters in patient-derived cells

As mitochondrial dysfunction is a key feature of cells from ALD patients,¹⁴ we further assessed this disease component. In untreated AMN fibroblasts, no clear phenotype of dysfunction was evident (Figure 2A). In contrast, in C-ALD fibroblasts, basal and ATP-linked OCR were reduced compared to healthy cells, by $-27%$

($p < 0.0001$) and $-44%$ ($p < 0.001$), respectively (Figure 2B). PXL065 treatment of C-ALD fibroblasts improved basal ($+29%$, $p < 0.0001$) and restored ATP-linked OCR (dedicated to ATP synthesis, $+100%$, $p < 0.0001$). Despite the lack of phenotype, PXL065 treatment also increased basal and ATP-linked OCR in AMN fibroblasts ($+7%$, $p < 0.001$ and $+87%$, $p < 0.05$, respectively). Maximal Oxidative Capacity (MOC) was consistently decreased across cell lines when compared to healthy cells; however small quantitative improvements mediated by PXL065 did not reach statistical

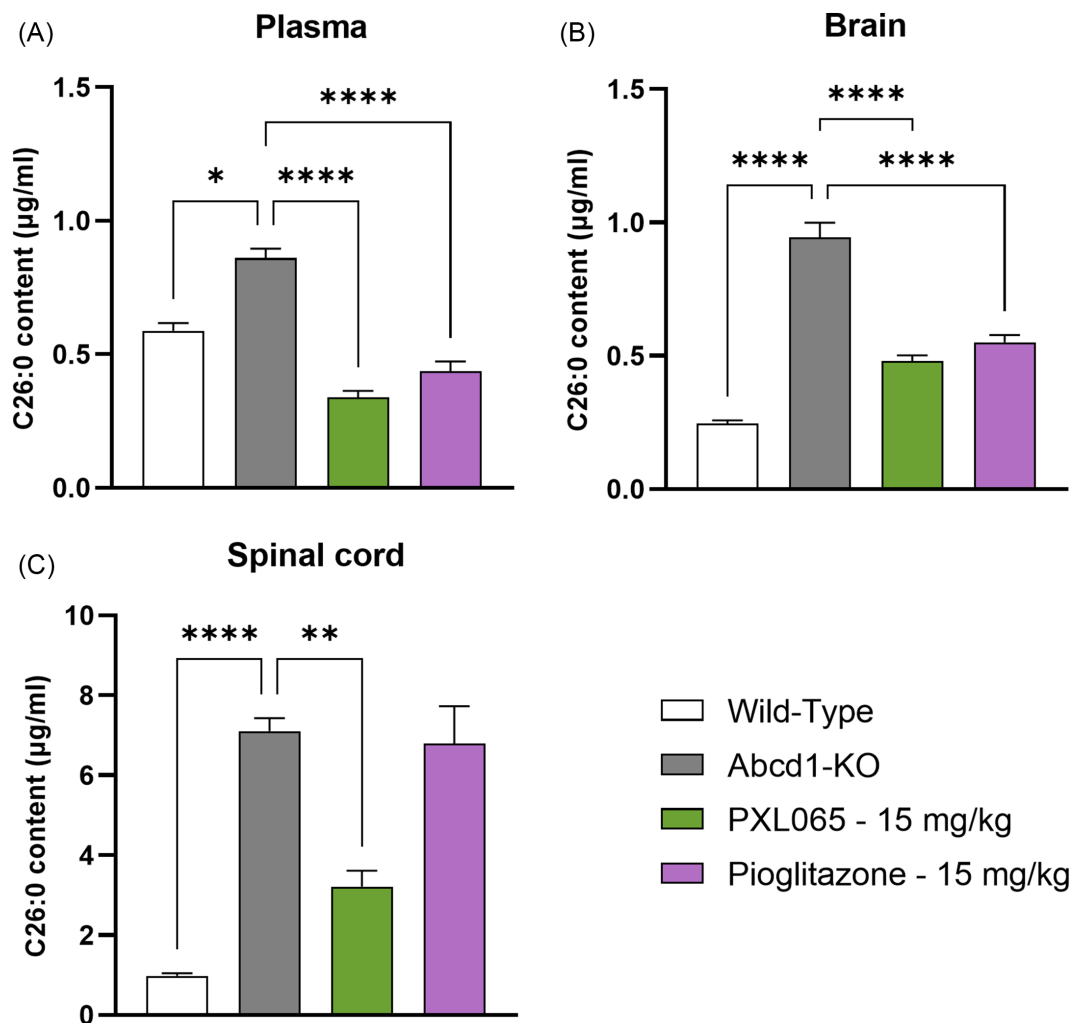


FIGURE 5 PXL065 reduces C26:0 levels in plasma, brain and spinal cord. Six-8-week-old *Abcd1*-null mice were treated with PXL065 or pioglitazone (15 mg/kg QD) for 8 weeks. C26:0 content was measured in plasma (A), brain (B) and spinal cord (C) by mass spectrometry. Results are mean \pm SEM, $n = 12$ wild-type, 15 untreated *Abcd1*-null, 15 PXL065 treated *Abcd1*-null and 15 pioglitazone treated *Abcd1*-null mice. * $p < 0.05$, ** $p < 0.01$, **** $p < 0.0001$ by one-way analysis of variance followed by Dunnett's multiple comparison or by Kruskal-Wallis followed by Dunn's multiple comparison versus untreated *Abcd1*-null mice

significance. Relative to PXL065, pioglitazone appeared to produce more limited effects on mitochondrial function. Similar results were observed in C-ALD lymphocytes (Figure S2).

Transporters related to ABCD1, namely ABCD2 and ABCD3, are reportedly able to subserve as alternative means of peroxisomal VLCFA import when ABCD1 is absent or deficient.¹⁵ We evaluated their expression by measuring mRNA levels following treatment with PXL065. No differences were observed in untreated patient—versus healthy cells (Figure 2C,D). In AMN fibroblasts, PXL065 induced the overexpression of ABCD2 by 15-fold ($p < 0.0001$), while ABCD3 increased by two-fold ($p < 0.001$) (Figure 2C). In C-ALD fibroblasts, PXL065-induced ABCD2 mRNA by three-fold, ($p < 0.01$) and ABCD3 by 2-fold ($p < 0.01$) (Figure 2D). Pioglitazone exhibited a similar profile in AMN and C-ALD fibroblasts. Similar results were observed in AMN lymphocytes (Figure S3).

3.3 | Effects in glial cells derived from *Abcd1*-null mice

As glial cell dysfunction and apoptosis are key defects in ALD,³ we evaluated the effects of compounds exposure in glial cells from *Abcd1*-null mice. As seen in patient-derived cells, C26:0 levels were markedly increased in diseased versus WT cells (Figure 3A). Both PXL065 (-92% , $p < 0.0001$) and pioglitazone (-87% , $p < 0.0001$) normalized C26:0 levels in *Abcd1*-null glial cells. Although no clear mitochondrial phenotype was observed in untreated cells from *Abcd1*-null mice (Figure 3B), basal and ATP-linked OCR were increased following PXL065 treatment, by $+58\%$ ($p < 0.01$) and $+31\%$ ($p < 0.01$), respectively, when compared to untreated cells. MOC was also increased by PXL065 treatment ($+63\%$, $p < 0.01$). Although pioglitazone tended to improve

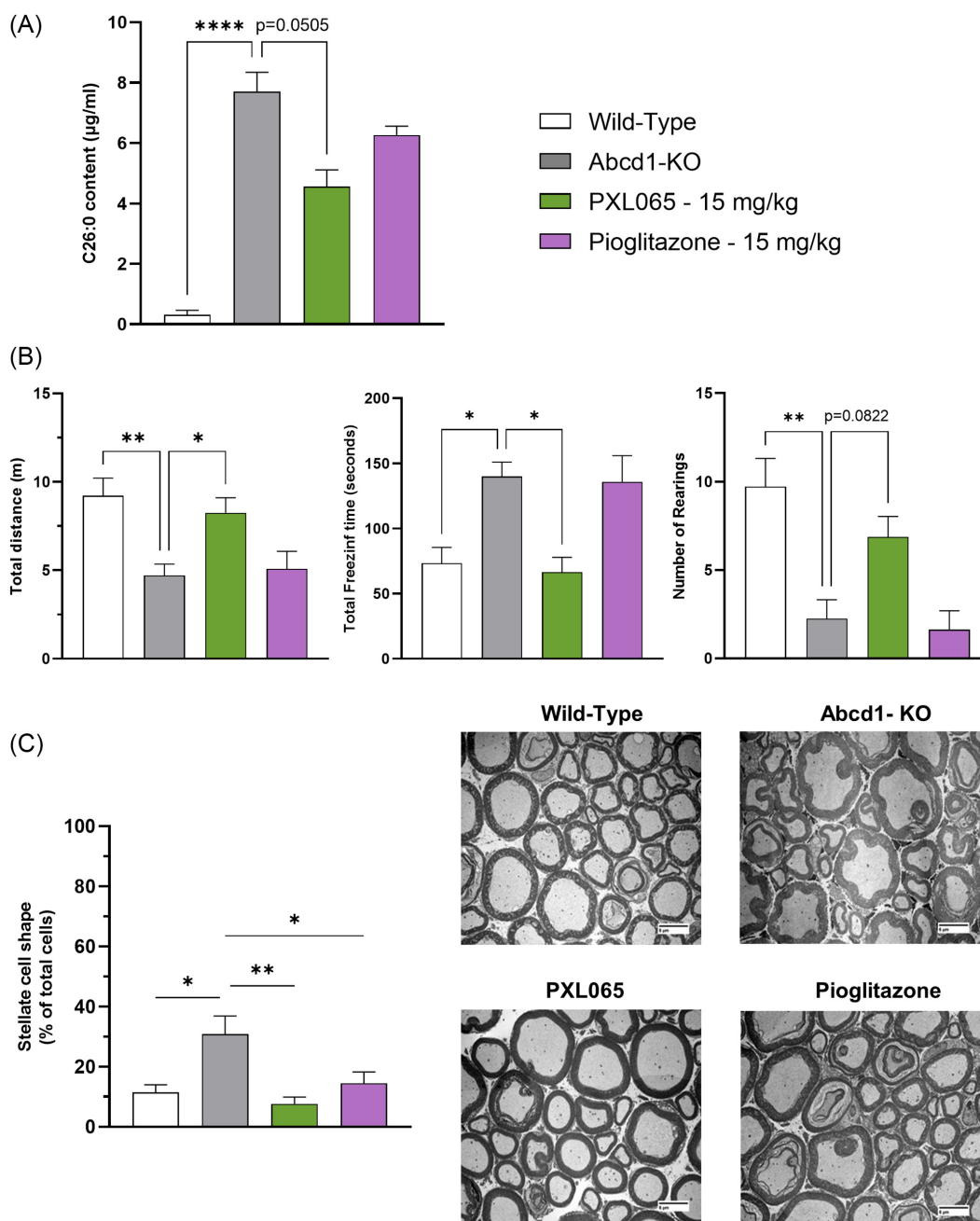


FIGURE 6 In older *Abcd1*-null mice, PXL065 lowers spinal cord very long chain fatty acids, improves sciatic nerve morphology and enhances neurobehavioral functions. Older (age 13 months) *Abcd1*-null mice were treated for 12 weeks with PXL065 or pioglitazone (15 mg/kg QD). (A) C26:0 content measured in spinal cord by mass spectrometry; results are mean \pm SEM, $n = 8$ animals/condition. (B) Open-field test monitoring results. Data are mean \pm SEM, $n = 8$ animals/condition (seven animals for wild-type in graph presenting number of rearings). (C) Axonal morphology (with representative images) of neurons determined by morphometric analysis of transversal slices of the sciatic nerve by electronic microscopy (800 \times). Data are mean \pm SEM, $n = 4$ animals/condition. * $p < 0.05$, ** $p < 0.01$, **** $p < 0.0001$ by one-way analysis of variance followed by Dunnett's multiple comparison or by Kruskal–Wallis followed by Dunn's multiple comparison vs untreated *Abcd1*-null mice

bioenergetic parameters, its effects did not reach statistical significance. Additionally, *Abcd2* and *Abcd3* mRNA levels were increased by PXL065 treatment of *Abcd1*-null glial cells but not by pioglitazone (Figure 3C).

3.4 | Effects on inflammatory gene expression profiles

In line with previous studies showing the role of inflammation in pathophysiology,¹⁶ C-ALD lymphocytes

TABLE 1 overview of the parameters measured and comparison between PXL065 and pioglitazone effects. Green identifies similar results between PXL065 and pioglitazone effects. Orange identifies different results

Parameter	Model	Effect of PXL065	Effect of pioglitazone	
In vitro	VLCFA	ALD cell lines	Decrease in C26:0 and C24:0	
		AMN fibroblasts	Decrease in C26:0 and C24:0	
Bioenergetics	ALD cell lines	C-ALD fibroblasts	Decrease in C26:0	
		AMN lymphocytes	Decrease in C26:0 and C24:0	
	Abcd1 null mice glial cells	C-ALD lymphocytes	Decrease in C26:0 and C24:0	
		AMN fibroblasts	Decrease in C26:0	
	ALD cell lines	AMN fibroblasts	Increase in basal and ATP-linked OCR	
		C-ALD fibroblasts	Increase in basal and ATP-linked OCR	
	Abcd1 null mice glial cells	C-ALD lymphocytes	Increase in basal, ATP-linked and maximal OCR	
		AMN fibroblasts	Increase in basal, ATP-linked and maximal OCR	
	ABCD2 – ABCD3 transporters	ALD cell lines	Increase in ABCD2 and ABCD3 expression	Increase in ABCD2 and ABCD3 expression
		C-ALD fibroblasts	Increase in ABCD2 and ABCD3 expression	Increase in ABCD2 expression only
Inflammation markers	AMN lymphocytes	Increase in ABCD2 and ABCD3 expression	Increase in ABCD2 and ABCD3 expression	
	C-ALD lymphocytes	No effect	No effect	
In vivo	VLCFA	Abcd1 null mice glial cells	Increase in ABCD2 and ABCD3 expression	
		C-ALD lymphocytes	Decrease in gene expression in multiple inflammatory markers	
Open field test	Stimulated Abcd1 null mice glial cells	6-8-week-old Abcd1-null mice	Decrease in gene expression in multiple inflammatory markers	
		13-month-old Abcd1-null mice	Decrease in gene expression in multiple inflammatory markers	
Sciatic nerve axon morphology	13-month-old Abcd1-null mice	6-8-week-old Abcd1-null mice	Decrease in C26:0 in plasma, brain, and spinal cord	
		13-month-old Abcd1-null mice	Decrease in C26:0 in plasma and brain	
Sciatic nerve axon morphology	13-month-old Abcd1-null mice	Open field test	No effect	
		Sciatic nerve axon morphology	No effect	
Sciatic nerve axon morphology	13-month-old Abcd1-null mice	Open field test	Decrease in stellate cell shape percentage	
		Sciatic nerve axon morphology	Decrease in stellate cell shape percentage	

Abbreviations: ALD, adrenoleukodystrophy; AMN, adrenomyeloneuropathy; C-ALD, cerebral-ALD; OCR, oxygen consumption rate; VLCFA, very long chain fatty acids.

exhibited increased expression of several pro-inflammatory genes (Figure 4A). Importantly, PXL065 was able to attenuate these increases; mean mRNA level reductions in NFκ-B (−66%, $p < 0.0001$), CCL5 (−81%, $p < 0.0001$) and NOS2 (−47%, $p < 0.0001$) were

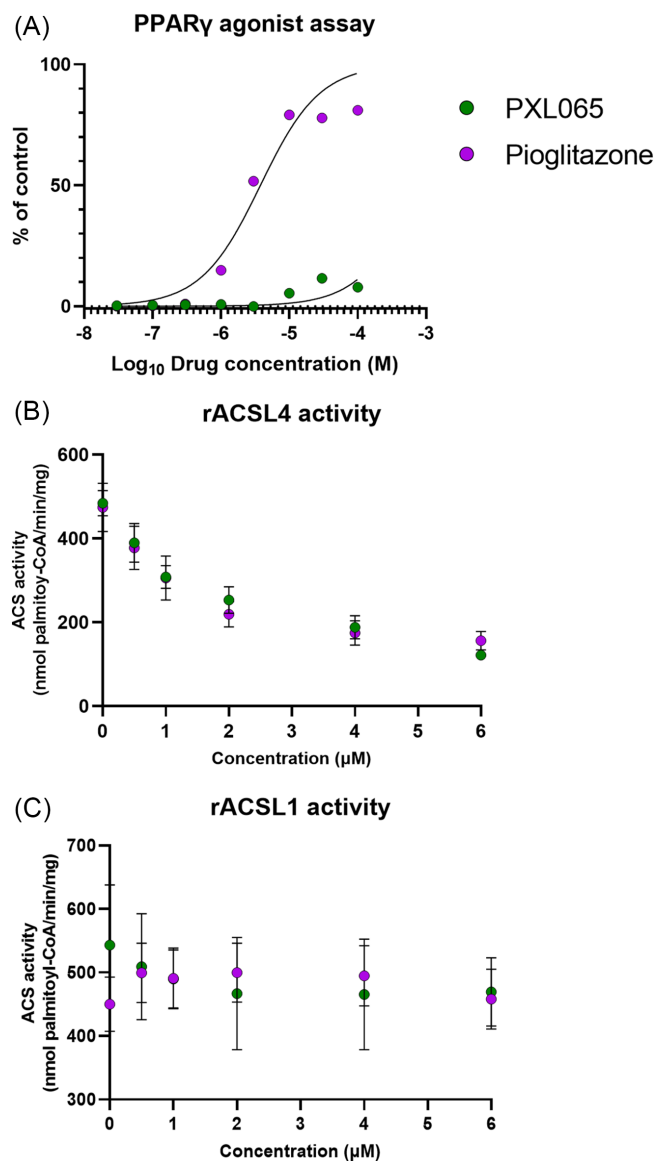


FIGURE 7 PXL065 retains nongenomic actions—inhibition of ACSL4—without PPAR γ agonist activity. Enzymatic activities were measured by ex situ biochemical assays. PPAR γ agonist activity (A) was measured using recombinant enzyme with a cofactor recruitment fluorescence assay using recombinant ligand binding domain protein in the presence of increasing concentrations of PXL065 or pioglitazone from 0.03 to 100 μ M. Results are expressed as a percent of the control response to 10 μ M rosiglitazone. ACSL4 (B) and ACSL1 activity (C) assays were performed using recombinant enzymes and [¹⁴C] palmitate, in the presence of increasing concentrations of PXL065, pioglitazone and leriglitazone from 0.5 to 6 μ M. Results are mean \pm SEM, $n = 3$ experiments for ACSL and 2 experiments for PPAR γ .

observed. Pioglitazone exhibited similar profiles (Figure 4A).

After stimulation with TNF α and IL1 β , a proinflammatory gene expression profile was also observed in Abcd1-null glial cells versus WT mouse glial cells (Figure 4B); this pattern was significantly improved by PXL065 and pioglitazone treatment. Several mRNAs encoding inflammatory mediators were significantly repressed: NFκB (−66%, $p < 0.01$), NOS2 (−63%, $p < 0.0001$), CCR2 (−55%, $p < 0.001$), CCR4 (−98%, $p < 0.0001$), and IL1b (−64%, $p < 0.0001$) (Figure 4B).

3.5 | PXL065 improves disease-associated phenotypes in Abcd1-null mice

Abcd1-null mice (6- to 8-week-old) were treated by oral gavage with PXL065 or pioglitazone at 15 mg/kg, once a day for 8 weeks (12 control WT, 15 untreated Abcd1 null, 15 PXL065-treated Abcd1 null and 15 pioglitazone-treated Abcd1-null mice). PXL065 significantly reduced elevated C26:0 by −61% ($p < 0.0001$) in plasma and by −49% ($p < 0.0001$) in brain (Figure 5A,B) when compared to untreated Abcd1-null mice. Pioglitazone decreased C26:0 by −48% ($p < 0.0001$) in plasma and by −42% ($p < 0.0001$) in

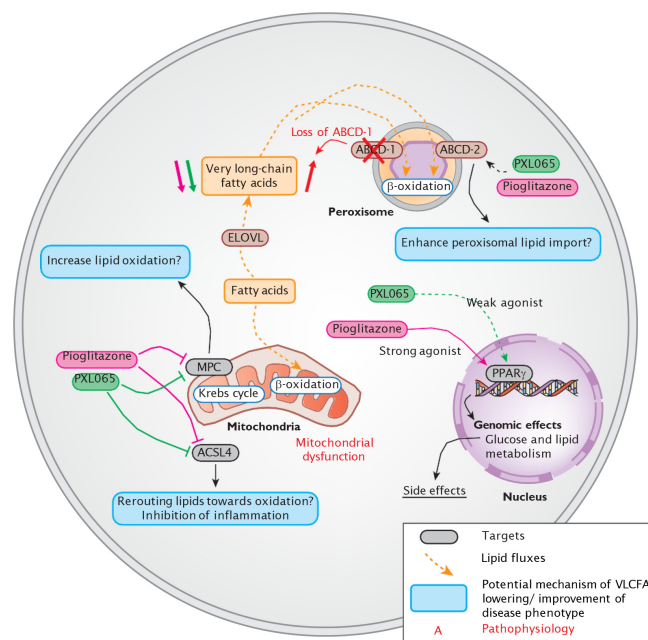


FIGURE 8 Diagram depicting the effects of PXL065 and Pioglitazone on PPAR γ , the mitochondrial pyruvate carrier (MPC) and ACSL4, and the associated pathways. Potential mechanisms linking the targets of the compounds of interest to very long chain fatty acids lowering and their efficacy on the disease phenotype are represented in the blue tags.

the brain. In spinal cord, PXL065—but not pioglitazone—decreased C26:0 by -55% ($p < 0.01$) (Figure 5C).

The neurologic phenotype of *Abcd1*-null mice is subtle and is generally only manifested in older mice.¹⁷ To interrogate the potential for in vivo efficacy in this context, 13-month-old *Abcd1*-null mice were treated orally with PXL065 or pioglitazone at the 15 mg/kg dose level for 12 weeks ($n = 8$ animals per condition). Similar to the effects observed in younger animals, spinal cord C26:0 content was elevated in untreated mice and was improved (-41% , $p = 0.0505$) by chronic PXL065 treatment (Figure 6A) while pioglitazone did not show any apparent effect.

Neurobehavioral functions were assessed using open-field test monitoring, a global assessment of spontaneous locomotor activity¹⁸ (eight animals per condition). At the end of the treatment period (i.e., at 16 months old), *Abcd1*-null mice exhibited impaired locomotor function, shown by a decrease of mean total distance traveled and number of rearings, and an increase in mean freezing time compared to age-matched WT mice (Figure 6B; seven animals for WT—number of rearings). Importantly, PXL065, but not pioglitazone, nearly normalized the mean total distance traveled ($p < 0.05$) and improved the mean freezing time ($p < 0.05$). Although not significant ($p = 0.08$), PXL065 tended to also increase the number of rearings. Altogether, these results indicate an improvement of locomotor function in the context of exploratory behavior in *Abcd1*-null mice treated with PXL065.

In this long-term study of older mice, sciatic nerve morphology was also assessed by EM (Figure 6C). An increase in the proportion of cells with an abnormal stellate shape ($+31\%$, $p < 0.05$) was noted in *Abcd1*-null mice compared to WT. Both PXL065 (-63% , $p < 0.01$) and pioglitazone (-37% , $p < 0.05$) significantly reduced the proportion of cells with stellate shape when compared to untreated mice.

The effects of PXL065 and pioglitazone on the different parameters measured in vitro and in vivo are summarized and compared in Table 1.

3.6 | Additional assessment of potential mechanisms

To further interrogate the potential molecular mechanism(s) of action of PXL065, we performed ex situ biochemical assays to measure the activity of the known targets of pioglitazone. We first confirmed its relative lack of PPAR γ agonism (Figure 7A). PPAR γ agonist potency was markedly greater for pioglitazone ($EC_{50} = 3.8 \mu\text{M}$) than for PXL065 ($EC_{50} > 100 \mu\text{M}$). Pioglitazone and other TZDs have previously been shown to inhibit a nongenomic target—

ACSL4, without any effect on the ACSL1 isoform.^{19,20} In in vitro ACS assays, both pioglitazone and PXL065 inhibited recombinant rat ACSL4 activity with the same potency ($IC_{50} = 2.08$ and $2.12 \mu\text{M}$, respectively) (Figure 7B). As expected, there was no inhibition of recombinant rat ACSL1 activity (Figure 7C). A visual summary of the targets of PXL065 and Pioglitazone is presented in Figure 7D.

4 | DISCUSSION

New therapeutic approaches for the treatment of patients with ALD are urgently needed to address the unmet medical needs associated with this debilitating monogenic neurometabolic disease. Although allogeneic hematopoietic stem cell transplantation was shown to be effective to treat C-ALD, it is a highly invasive procedure that is not without risks, such as graft failure and infections from opportunistic pathogens.²¹ Of note, the procedure yields more favorable outcomes in the context of early-stage disease.²¹

PXL065 is a novel TZD and the deuterium-stabilized (*R*)-enantiomer of pioglitazone that is currently in Phase 2 clinical development for non-alcoholic steatohepatitis (NASH, [ClinTrials.Gov](https://clinicaltrials.gov/ct2/show/study/NCT04321343) ID:NCT04321343). Since pioglitazone has been reported to ameliorate features of ALD in preclinical models,⁹ we sought to test the hypothesis that PXL065 could also be an attractive therapeutic candidate for ALD.

In a series of in vitro experiments in two ALD cells lines derived from one AMN and one C-ALD patient, PXL065 improved multiple disease-related phenotypes. Remarkably, PXL065 nearly normalized elevated C26:0 content. These effects were accompanied by a reduction of elevated C24:0 levels without changing the levels of C22:0, suggesting specificity to the VLCFA species that are associated with ALD.² Of note, the molecular mechanisms linking PXL065 to the VLCFA lowering we observed are yet to be determined. Further experiments would be required to decipher whether suppression of very long chain fatty acid elongase and/or conversion to monounsaturated forms and/or improved β -oxidation are at play.

Mitochondrial dysfunction is described as a key component of the pathophysiology, which could contribute to the clinical onset through a decrease in β -oxidation activity.²² VLCFA-induced cytotoxicity is also reported to target cellular energy-dependent functions.²³ In addition, ultrastructural examination of neural tissue from AMN patients also reveals abnormal mitochondria.²⁴ Increased ATP-linked OCR mediated by PXL065 could contribute to preserving a broader range of cellular energy-dependent functions altered in the disease. Although

VLCFA catabolism is mostly mediated by peroxisomes, we speculate that increased OCR in response to PXL065 might enhance mitochondrial lipid oxidation and contribute to VLCFA lowering by driving catabolism of shorter chain length fatty acid precursors that are substrates for the elongase that catalyzes synthesis of C24:0 and C26:0.²⁵ Overall, an increase in mitochondrial efficiency mediated by PXL065 could support essential cellular functions and participate in global phenotypic improvements.

Although somewhat controversial,²⁶ current evidence indicates that ABCD2 (and ABCD3) have VLCFA transport capacity and could compensate for the absence of ABCD1.^{15,27} Thus, overexpression of ABCD2 has been proposed as a therapeutic approach for ALD.^{28,29} The increased expression of ABCD2 induced by PXL065 might, therefore, contribute to lower VLCFA levels found in patient-derived cells. Although we did not assess this hypothesis in vivo, ex vivo data obtained in glial cells from *Abcd1*-null mice provide further support for this potential mechanism.

Cerebral ALD is characterized by an important inflammatory component.³⁰ The transition to overt C-ALD is not well understood but might involve low-grade inflammation with environmental triggers leading to uncontrolled inflammation. Of interest, TZD's (including pioglitazone) were reported to attenuate cytokine production by human immune cells³¹ and to protect from neuroinflammation via effects on peroxisomes.³² Accordingly, our results showed that PXL065 has the potential to repress pro-inflammatory gene expression in *Abcd1*-null mouse-derived glial cells and C-ALD patient-derived lymphocytes. Although we did not assess this parameter in vivo, PXL065 was previously shown to attenuate inflammation in vivo in the *db/db* mouse model of metabolic syndrome.¹¹

The most widely used in vivo model of ALD is the *Abcd1*-null mouse. This model exhibits a phenotype consistent with AMN, including increased VLCFA levels in plasma and tissues beginning at an early age³³ as well as the later development of neurological impairment.¹⁷ In this context, PXL065 reduced elevated VLCFA in plasma, spinal cord and brain. In addition, PXL065 ameliorated impaired locomotor function in 13-month-old mice, suggesting an improvement of the progression of neurologic dysfunction. This effect coincided with reduced VLCFA in spinal cord but may also have resulted from additional positive effects on mitochondrial function, as demonstrated ex vivo, for instance. Importantly, PXL065 treatment improved the proportion of abnormally shaped axons in sciatic nerve from *Abcd1*-null mice. This feature has not been previously reported in mice. However, there are reports of similar findings in peripheral nerve and

dorsal root ganglia from patients with AMN including swelling of individual axons, lamellar changes in myelin and segmental demyelination.³⁴ On balance, the in vivo efficacy achieved with PXL065 in two independent long-term studies in *Abcd1*-null mice further supports the pursuit of this compound as a possible therapy for ALD.

The beneficial effects observed with PXL065 appeared to be superior to pioglitazone for several parameters at the same concentrations and doses (see comparison in Table 1). Differences included: improvements in mitochondrial function in patient-derived and mouse glial cells, *Abcd2* and *Abcd3* mRNA induction in diseased glial cells, reductions in spinal cord VLCFA levels, and effects on all three main parameters measured in the open-field test. In the more severe *Abcd1/Abcd2* double knockout model, Morato et al.⁹ reported that pioglitazone improved axonal degeneration and locomotor deficits without significantly impacting VLCFA levels. Reasons for the latter discrepancy are uncertain although a lower (9 mg/kg/day) dose of pioglitazone was employed and administered in the diet instead of by oral gavage. Leriglitazone is a related TZD, also derived from pioglitazone, which is in clinical development in ALD patients (ClinTrials.gov ID: NCT03231878). In both *Abcd1*-null and *Abcd1/Abcd2* double knockout mice, leriglitazone exerted efficacy including evidence of reduced oxidative stress, improved mitochondrial function and improved motor function.¹⁰ Of interest, leriglitazone was not reported to significantly affect plasma VLCFA; in vivo.¹⁰

As illustrated in Figure 8, unlike pioglitazone or leriglitazone, PXL065 has minimal intrinsic PPAR γ agonist activity. However, molecular mechanisms underlying its observed beneficial effects in ALD models may still include residual PPAR γ action since partial conversion of (*R*)- (PPAR γ inactive) to (*S*)- (PPAR γ active) pioglitazone occurs between dosing intervals in cell culture and in vivo.¹¹ Nevertheless, after repeated administration, steady-state ratios of R:S enantiomers achieved with PXL065 are substantially (four- to eight-fold) greater than those seen with pioglitazone—including in human subjects.¹¹ In addition, we previously demonstrated a lack of PPAR γ -mediated effects in vivo in mice (weight gain, fluid retention, or increases in adiponectin) at the same dose level of PXL065 (15 mg/kg) that was used in *Abcd1*-null mice here.¹¹ Therefore, we envision that the efficacious dose levels of PXL065 could potentially be achieved in patients with ALD without the known liabilities of weight gain, edema, and bone loss that are mediated by stronger PPAR γ agonism (as illustrated in Figure 8).

Apart from PPAR γ , TZDs (including pioglitazone) modulate two distinct nongenomic pathways (as illustrated in Figure 8). We previously demonstrated that PXL065 inhibits MPC with a potency equivalent to pioglitazone—

IC₅₀'s 7–9 μM ,¹¹ and leriglitazone also inhibits MPC with an IC₅₀ of 4.1 μM .³⁵ Selective inhibition or genetic deletion of MPC is known to reduce intracellular lipid accumulation and inflammation in fatty liver disease models.^{36,37} Such effects could potentially also be relevant in the context of ALD pathophysiology. Of greater potential importance, a specific MPC inhibitor was also shown to exert efficacy in models of neurodegeneration—specifically, to reduce neuroinflammation and improve locomotor function in Parkinson's disease models.³⁸

In the present study, we also determined that, like pioglitazone,²⁰ PXL065 serves as a selective in vitro inhibitor of purified ACSL4 (vs. ACSL1) activity (as illustrated in Figure 8). ACSL4 is expressed in multiple tissues including brain and adrenal, which are affected in ALD.³⁹ ACSL4's preferred substrates include unsaturated lipids (PUFA, HUFA) lipids (e.g. arachidonic acid),⁴⁰ which are distinct from saturated VLCFA (e.g. C26:0). However, ACSL4 is implicated broadly in lipid channeling in cells.⁴¹ For example in an in vivo model, ACSL4 activity was shown to be important in regulating the incorporation of arachidonic acid into phospholipids as well as the downstream effects of diet-induced obesity, including adipose tissue inflammation.⁴¹ Most importantly, ACSL4 is now well established as a major driver of lipid peroxidation-mediated and iron-dependent cell death, or ferroptosis.^{42,43} TZD-mediated inhibition of ferroptosis was shown to be tissue-protective in the setting of pulmonary ischemia.⁴⁴ Moreover, knockdown of ACSL4 protected mice against brain ischemia and neuroinflammation, whereas, forced overexpression of ACSL4 reportedly exacerbated ischemic brain injury.⁴⁵ Ferroptosis is now being increasingly considered as a component of several neurodegenerative diseases.^{43,46} Although no link between ALD pathophysiology and ferroptosis or ACSL4 has been established to-date, we speculate that inhibition of ACSL4 might also contribute to long-term beneficial effects of PXL065 (or pioglitazone) to attenuate neuroinflammation or neuronal cell loss in the context of ALD. Future studies will be required to further assess if or how inhibition of either MPC or ACSL4—versus residual PPAR γ agonist activity—could impact cellular VLCFA accumulation or downstream features of ALD pathophysiology.

In the present series of experiments, we characterized PXL065 in well-accepted preclinical models of ALD and demonstrated that it has the potential to suppress VLCFA accumulation, the proximate driver of disease, and to also attenuate other features of disease pathophysiology. The in vivo efficacy profile of PXL065 also suggests that clinical development could proceed by first assessing effects on biomarkers of disease followed by long-term trials designed to confirm clinical benefits. A clinical development program that is initially focused on adult patients with AMN is planned to begin in 2022.

AUTHOR CONTRIBUTIONS

Pierre-Axel Monternier, Jaspreet Singh, Eric Klett, David E. Moller, and Sophie Hallakou-Bozec designed the experiments, analyzed results, and participated to the writing of the manuscript. **Parveen Parasar, Navtej Kaur, and Tavarekere N. Nagaraja** performed the experiments. **Pierre Theurey, Sheila DeWitt, and Vincent Jacques** participated to the writing of the manuscript.

ACKNOWLEDGMENT

The authors thank Jun Xu for technical help with in vivo studies.

FUNDING

This work was supported by funds from Poxel. Jaspreet Singh is also supported by National Institute of Health grants NS114245 and NS114775. Navtej Kaur is supported by funds from Henry Ford Health System.

CONFLICT OF INTEREST

Pierre-Axel Monternier is an employee and shareholder of Poxel. Jaspreet Singh received sponsored research grants from Poxel to support the conduct of experiments related to the aims of this manuscript and is also a member of Poxel's Scientific Advisory Board. Parveen Parasar declares no conflict of interest. Pierre Theurey is an employee and shareholder of Poxel. Sheila DeWitt received sponsored research grants from Poxel to support the conduct of experiments related to the aims of this manuscript. Vincent Jacques received sponsored research grants from Poxel to support the conduct of experiments related to the aims of this manuscript. Eric Klett received sponsored research grants from Poxel to support the conduct of experiments related to the aims of this manuscript. Navtej Kaur declares no conflict of interest. Tavarekere N. Nagaraja declares no conflict of interest. David E. Moller is an employee and shareholder of Poxel. Sophie Hallakou-Bozec is an employee and shareholder of Poxel.

DATA AVAILABILITY STATEMENT

The data that support the findings of this study are available from the corresponding author upon reasonable request.

ORCID

Pierre Theurey  <https://orcid.org/0000-0001-8885-0648>

REFERENCES

1. Moser HW, Mahmood A, Raymond GV. X-linked adrenoleukodystrophy. *Nat Clin Pract Neurol*. 2007;3(3):140-151.
2. Moser HW, Moser AB, Frayer KK, et al. Adrenoleukodystrophy. Increased plasma content of saturated very long chain fatty acids. *Neurology*. 1981;31(10):1241.

3. Eichler FS, Ren JQ, Cossoy M, et al. Is microglial apoptosis an early pathogenic change in cerebral X-linked adrenoleukodystrophy? *Ann Neurol*. 2008;63(6):729-742.
4. Hein S, Schonfeld P, Kahlert S, Reiser G. Toxic effects of X-linked adrenoleukodystrophy-associated, very long chain fatty acids on glial cells and neurons from rat hippocampus in culture. *Hum Mol Genet*. 2008;17(12):1750-1761.
5. Fourcade S, Lopez-Erauskin J, Galino J, et al. Early oxidative damage underlying neurodegeneration in X-adrenoleukodystrophy. *Hum Mol Genet*. 2008;17(12):1762-1773.
6. Galino J, Ruiz M, Fourcade S, et al. Oxidative damage compromises energy metabolism in the axonal degeneration mouse model of X-adrenoleukodystrophy. *Antioxid Redox Signal*. 2011;15(8):2095-2107.
7. Fourcade S, López-Erauskin J, Ruiz M, Ferrer I, Pujol A. Mitochondrial dysfunction and oxidative damage cooperatively fuel axonal degeneration in X-linked adrenoleukodystrophy. *Biochimie*. 2014;98:143-149.
8. Engelen M, Kemp S, De Visser M, et al. X-linked adrenoleukodystrophy (X-ALD): clinical presentation and guidelines for diagnosis, follow-up and management. *Orphanet J Rare Dis*. 2012;7(1):51.
9. Morato L, Galino J, Ruiz M, et al. Pioglitazone halts axonal degeneration in a mouse model of X-linked adrenoleukodystrophy. *Brain*. 2013;136(Pt 8):2432-2443.
10. Rodríguez-Pascau L, Vilalta A, Cerrada M, et al. The brain penetrant PPAR γ agonist leriglitazone restores multiple altered pathways in models of X-linked adrenoleukodystrophy. *Sci Transl Med*. 2021;13(596):eabc0555.
11. Jacques V, Bolze S, Hallakou-Bozec S, et al. Deuterium-stabilized (R)-pioglitazone (PXL065) is responsible for pioglitazone efficacy in NASH yet exhibits little to no PPAR γ activity. *Hepatol Commun*. 2021;5(8):1412-1425.
12. Singh J, Giri S. Loss of AMP-activated protein kinase in X-linked adrenoleukodystrophy patient-derived fibroblasts and lymphocytes. *Biochem Biophys Res Commun*. 2014;445(1):126-131.
13. Singh J, Khan M, Singh I. Silencing of *Abcd1* and *Abcd2* genes sensitizes astrocytes for inflammation: implication for X-adrenoleukodystrophy. *J Lipid Res*. 2009;50(1):135-147.
14. Baarine M, Beeson C, Singh A, Singh I. ABCD1 deletion-induced mitochondrial dysfunction is corrected by SAHA: implication for adrenoleukodystrophy. *J Neurochem*. 2015;133(3):380-396.
15. Netik A, Forss-Petter S, Holzinger A, Molzer B, Unterrainer G, Berger J. Adrenoleukodystrophy-related protein can compensate functionally for adrenoleukodystrophy protein deficiency (X-ALD): implications for therapy. *Hum Mol Genet*. 1999;8(5):907-913.
16. Lund TC, Stadem PS, Panoskaltis-Mortari A, et al. Elevated cerebral spinal fluid cytokine levels in boys with cerebral adrenoleukodystrophy correlates with MRI severity. *PLoS One*. 2012;7(2):e32218.
17. Pujol A, Hindelang C, Callizot N, Bartsch U, Schachner M, Mandel JL. Late onset neurological phenotype of the X-ALD gene inactivation in mice: a mouse model for adrenomyeloneuropathy. *Hum Mol Genet*. 2002;11(5):499-505.
18. Yanai S, Endo S. Functional aging in male C57BL/6J mice across the life-span: a systematic behavioral analysis of motor, emotional, and memory function to define an aging phenotype. *Front Aging Neurosci*. 2021;13:697621.
19. Askari B, Kanter JE, Sherrid AM, et al. Rosiglitazone inhibits acyl-CoA synthetase activity and fatty acid partitioning to diacylglycerol and triacylglycerol via a peroxisome proliferator-activated receptor-gamma-independent mechanism in human arterial smooth muscle cells and macrophages. *Diabetes*. 2007;56(4):1143-1152.
20. Kim JH, Lewin TM, Coleman RA. Expression and characterization of recombinant rat acyl-CoA synthetases 1, 4, and 5. Selective inhibition by triacsin C and thiazolidinediones. *J Biol Chem*. 2001;276(27):24667-24673.
21. Raymond GV, Aubourg P, Paker A, et al. Survival and functional outcomes in boys with cerebral Adrenoleukodystrophy with and without hematopoietic stem cell transplantation. *Biol Blood Marrow Transplant*. 2019;25(3):538-548.
22. McGuinness MC, Lu JF, Zhang HP, et al. Role of ALDP (ABCD1) and mitochondria in X-linked Adrenoleukodystrophy. *Mol Cell Biol*. 2003;23(2):744-753.
23. Kruska N, Schönfeld P, Pujol A, Reiser G. Astrocytes and mitochondria from adrenoleukodystrophy protein (ABCD1)-deficient mice reveal that the adrenoleukodystrophy-associated very long-chain fatty acids target several cellular energy-dependent functions. *Biochim Biophys Acta*. 2015;1852(5):925-936.
24. Powers JM, Deciero DP, Cox C, et al. The dorsal root ganglia in adrenomyeloneuropathy: neuronal atrophy and abnormal mitochondria. *J Neuropathol Exp Neurol*. 2001;60(5):493-501.
25. Ofman R, Dijkstra IME, Van Roermund CWT, et al. The role of ELOVL1 in very long-chain fatty acid homeostasis and X-linked adrenoleukodystrophy. *EMBO Mol Med*. 2010;2(3):90-97.
26. Maier EM, Mayerhofer PU, Asheuer M, et al. X-linked adrenoleukodystrophy phenotype is independent of ABCD2 genotype. *Biochem Biophys Res Commun*. 2008;377(1):176-180.
27. Pujol A, Ferrer I, Camps C, et al. Functional overlap between ABCD1 (ALD) and ABCD2 (ALDR) transporters: a therapeutic target for X-adrenoleukodystrophy. *Hum Mol Genet*. 2004;13(23):2997-3006.
28. Fourcade S, Savary S, Albet S, et al. Fibrate induction of the adrenoleukodystrophy-related gene (ABCD2). *Eur J Biochem*. 2001;268(12):3490-3500.
29. Fourcade S, Savary S, Gondcaille C, et al. Thyroid hormone induction of the adrenoleukodystrophy-related gene (ABCD2). *Mol Pharmacol*. 2003;63(6):1296-1303.
30. Powers JM, Liu Y, Moser AB, Moser HW. The inflammatory myelinopathy of adreno-leukodystrophy: cells, effector molecules, and Pathogenetic implications. *J Neuropathol Exp Neurol*. 1992;51(6):630-643.
31. Zhang WY, Schwartz EA, Permana PA, Reaven PD. Pioglitazone inhibits the expression of inflammatory cytokines from both monocytes and lymphocytes in patients with impaired glucose tolerance. *Arterioscler Thromb Vasc Biol*. 2008;28(12):2312-2318.
32. Gray E, Ginty M, Kemp K, Scolding N, Wilkins A. The PPAR-gamma agonist pioglitazone protects cortical neurons from inflammatory mediators via improvement in peroxisomal function. *J Neuroinflammation*. 2012;9(1):63.

33. Lu J-F, Lawler AM, Watkins PA, et al. A mouse model for X-linked adrenoleukodystrophy. *Proc Natl Acad Sci.* 1997;94(17):9366-9371.
34. Powers JM. Adreno-leukodystrophy (adreno-testiculo-leukomyelo-neuropathic-complex). *Clin Neuropathol.* 1985;4(5):181-199.
35. Patent WO/2019/234690. Use of 5-[[4-[2-[5-acetylpyridin-2-yl]ethoxy]benzyl]-1,3-thiazolidine-2,4-dione and its salts. 2019.
36. Rauckhorst AJ, Gray LR, Sheldon RD, et al. The mitochondrial pyruvate carrier mediates high fat diet-induced increases in hepatic TCA cycle capacity. *Mol Metab.* 2017;6(11):1468-1479.
37. McCommis KS, Hodges WT, Brunt EM, et al. Targeting the mitochondrial pyruvate carrier attenuates fibrosis in a mouse model of nonalcoholic steatohepatitis. *Hepatology.* 2017;65(5):1543-1556.
38. Ghosh A, Tyson T, George S, et al. Mitochondrial pyruvate carrier regulates autophagy, inflammation, and neurodegeneration in experimental models of Parkinson's disease. *Sci Transl Med.* 2016;8(368):368ra174.
39. Grevenkoed TJ, Klett EL, Coleman RA. Acyl-CoA metabolism and partitioning. *Annu Rev Nutr.* 2014;34:1-30.
40. Klett EL, Chen S, Yechoor A, Lih FB, Coleman RA. Long-chain acyl-CoA synthetase isoforms differ in preferences for eicosanoid species and long-chain fatty acids. *J Lipid Res.* 2017;58(5):884-894.
41. Killion EA, Reeves AR, el Azzouny MA, et al. A role for long-chain acyl-CoA synthetase-4 (ACSL4) in diet-induced phospholipid remodeling and obesity-associated adipocyte dysfunction. *Mol Metab.* 2018;9:43-56.
42. Doll S, Proneth B, Tyurina YY, et al. ACSL4 dictates ferroptosis sensitivity by shaping cellular lipid composition. *Nat Chem Biol.* 2017;13(1):91-98.
43. Li J, Cao F, Yin HL, et al. Ferroptosis: past, present and future. *Cell Death Dis.* 2020;11(2):88.
44. Xu Y, Li X, Cheng Y, Yang M, Wang R. Inhibition of ACSL4 attenuates ferroptotic damage after pulmonary ischemia-reperfusion. *FASEB J.* 2020;34(12):16262-16275.
45. Cui Y, Zhang Y, Zhao X, et al. ACSL4 exacerbates ischemic stroke by promoting ferroptosis-induced brain injury and neuroinflammation. *Brain Behav Immun.* 2021;93:312-321.
46. Viktorinova A, Durfinova M. Mini-review: is iron-mediated cell death (ferroptosis) an identical factor contributing to the pathogenesis of some neurodegenerative diseases? *Neurosci Lett.* 2021;745:135627.

SUPPORTING INFORMATION

Additional supporting information may be found in the online version of the article at the publisher's website.

How to cite this article: Monternier P-A, Singh J, Parasar P, et al. Therapeutic potential of deuterium-stabilized (*R*)-pioglitazone—PXL065—for X-linked adrenoleukodystrophy. *J Inherit Metab Dis.* 2022;45(4):832-847. doi:10.1002/jimd.12510